Effects of random migration in population dynamics

Alexandre Colato* and Salomon S. Mizrahi†
Departamento de Física, CCET, Universidade Federal de São Carlos, Rodovia Washington Luiz km 235, São Carlos, 13565-905, SP, Brazil

(Received 13 November 2000; revised manuscript received 23 March 2001; published 8 June 2001)

We study the influence of random migration of a species (may be insects) in the population dynamics when initially all the individuals live in a *primordial site* (their habitats may be trees). We assume (i) a finite number of sites, (ii) that migration occurs randomly to nearest neighbors, and (iii) an on-site age-structured population whose size varies according to Ricker's map. We find that even for a very small migration rate, the population density becomes appreciably affected. If migration is not allowed, depending on the value of the characteristic parameters, the population may display a chaotic oscillation; however, with migration permitted, the chaos is reduced or even suppressed, and the population density will oscillate with period 2 or period 4. We examined the effects of migration through higher-order iterations of the map, entropy, and time correlation function. We also considered a long chain, analyzing (a) the spatial correlation between sites, noting the occurrence of a transition in the correlation function between sites separated by odd and even units of distance and (b) the fluctuations in time of the populations when initially all sites are populated.

DOI: 10.1103/PhysRevE.64.011901 PACS number(s): 87.23.Cc, 87.10.+e, 02.30.Oz, 02.70.Bf

I. INTRODUCTION

The proposal by Malthus [1] of a population dynamics model, by which the human population shows a tendency to grow geometrically whereas food production should increase arithmetically, was a stimulus for later investigators to develop mathematical models to express a population variation as function of time, not only in humans but also in other species of animals and plants. For instance, in 1844 Verhulst proposed a logistic differential equation for population growth [2]. Thereafter other models were proposed, which could be verified from the observation of population size of species in the wild or under controlled laboratory conditions. Modeling in population dynamics consists in proposing a mechanism that can be expressed as an equation having the capacity to either retrodict the population changes along the preceding days, years or generations, and/or for predicting the evolution of its size from previously collected data. The equation should contain one or more parameters (to express birth rate, death rate, etc.) and it can be either differential (when time is continuous) or of finite differences (time is discrete). In the later case, a unit of time is usually considered to be the lapse between two consecutive generations (it is said to be age structured). Age-structured population can be found in arthropod species with one short-lived adult generation per year [3], insects having a summer and a winter generation [4].

A trivial and illustrative model for population growth, although unrealistic, goes as follows: start with one pair of rabbits (one male and one female) that reproduce after N days (time unit), the female gives birth to one pair of newborns (again, one male and one female) constituting the second generation of rabbits and a female can reproduce only twice during the span of her life. The second generation will also reproduce after N days and only twice too, and so on with the following generations. This parameter-free model gives a pedagogical view of the trend of the population growth of the females; so a linear equation can represent the model: $P_{n+1}=P_n+P_{n-1}$ with initial conditions $P_0=P_1=1$, which generates the sequence of Fibonacci numbers, 1,1,2,3,5,8,13,$\cdots$.

Realistically, many factors influence the evolution of a population size, for instance, the environment being favorable or not (temperature, level of hazardous radiation, raining season, etc.), abundance or scarcity of food, effect of predators, parasites, diseases, etc. Real situations show that in order to describe adequately a population dynamics, the equations should be nonlinear; a nonlinear equation may display fixed points, cyclic variation or even chaotic oscillations of the population, depending on the values of the parameters.

Models describing the variation of an age-structured population lead to equations of the general nonlinear form,

$$P_{n+1}=R(P_n)P_n. \tag{1}$$

Usually the function $R(P_n)$ is not complicated, but the analytical determination of the population size P_n may not be a trivial task, and one has to resort to numerical calculations. However before going to a computer, it is possible to make some qualitative analysis of the model [5].

The fixed points P_* (attractors, repellers, etc.) in Eq. (1) give the kind of stability (or instability), the population size may attain at the long. The fixed points are determined by solving the equation $R(P_*)=1$ (there is also the trivial solution, $P_*=0$). The stability in the neighborhood of the fixed point is determined by analyzing the eigenvalue $\lambda \equiv d[R(P)P]/dP|_{P=P_*}$ and the location of the point of maximum P_m of the curve $R(P)P$, thus the following cases are possible: (a) if $P_m>P_*$ and $0<\lambda<1$ then P_* is a stable fixed point (an attractor) and $P_n \to P_*$ monotonically. (b) When $P_m<P_*$ four situations may happen where P_n oscillates around P_*: (b1) if $-1<\lambda<0$ the fixed point P_* is a

*Email address: colato@ifsc.sc.usp.br
†Email address: salomon@df.ufscar.br

stable equilibrium point (an attractor) and $P_n \to P_*$ with damped oscillations; (b2) for $\lambda = -1$ the fixed point is neutrally stable, asymptotically the P_n remain oscillating around P_* but $P_n \not\to P_*$ (pitchfork bifurcation); (b3) when $\lambda < -1$ or $\lambda > 1$, the fixed point is unstable (a repeller), the oscillations of P_n are erratic but never surpass P_m; (b4) a tangent bifurcation might occur at $\lambda = 1$.

For instance, the initial population size of a strain of bacteria immersed in a favorable medium of nutrients may double at each unit interval of time T; however, when the population becomes large enough and the medium is not anymore sufficiently favorable for allowing the population to double in size indefinitely at the same rate, it will eventually saturate at some value. Saturating population models were introduced by Verhulst, as an example let us consider [6]

$$R(P_n) = \frac{2}{1 + \dfrac{P_n}{K}}. \tag{2}$$

The fixed point is $P_* = K$, the eigenvalue is $\lambda = 1/2$, and there is no point of maximum, however, the saturation value of $xR(x)$ is $2K$; therefore P_* is an attractor and $P_n \to P_*$, monotonically. Indeed, an exact solution can be obtained by a linearization transformation: writing $P_n = 1/Q_n$, Eq. (2) becomes linear, therefore solvable exactly, see Ref. [7]. Although non-linearizable unimodal maps may show a chaotic oscillation. Its very existence in natural populations, as a general trend is still controversial. However there is some evidence that it exists in some pest insects [8,9]. The occurrence of chaotic fluctuation in pest insects is a highly desirable behavior since recent developments in dynamical systems theory allow chaos control and this could be used to restrain the insect population growth [10]. In another study of population dynamics, it was shown that a system that is chaotic under constant environmental conditions may become ordered if the conditions change periodically or randomly [11].

Unimodal maps like Eq. (1) describe global population changes (P_n stands for the population or its density when normalization is carried out) without distinguishing between groups scattered among several sites. However, contact between individuals (living in different sites) through migration exist and the effects on the population size, at each site, may be quite remarkable. Chaos and migration in a dynamic population model were studied in Ref. [12]. The authors considered an age-structured group of spatially interbreeding populations (a metapopulation) linked by migration and subject to environmental disturbance (local and global noises) and showed that although low densities lead to a more frequent extinction at some sites (local site), the decorrelating effect of chaotic oscillations reduces the degree of sincrony among populations, thus impeding the whole population extinction. When a population in a site goes extinct, recolonization by migration prevents global extinction. Other approaches can be found in Refs. [13–18].

In this paper, we report our study of the case of a single species whose population concentrates initially in a special site, the *primordial site*, of a one-dimensional (1D) chain, with all other sites not yet settled. Then the individuals are allowed to emigrate to neighboring sites according to the so-called *random walk model* or to remain in the same site. The same happens with the other sites as they become populated. We analyze the dynamical effects of this migration on the population density at each site; the population dynamics is assumed to be ruled by Ricker's map [19]. We verify that even for a very small migration rate the population of the sites are highly affected in their dynamics, for instance, at regimes of chaotic oscillations the migration suppresses the chaos, making the population size to oscillate with period 2 or period 4. For a long chain of sites, we analyze (a) the spatial correlation between sites, noting the occurrence of a transition in the correlation function between sites separated by odd and even units of distance, and (b) the fluctuations in time of the populations when initially all sites are populated, noting that it takes much more time to stabilize the fluctuations in case when growth is allowed in the primordial site only than in the case growth occurs in all sites simultaneously.

This paper contains four additional sections and it is organized as follows: In Sec. II we present the random migration equation coupled to Ricker's map for describing the population on-site variation. In Sec. III one analyzes the effects of migration through the higher-order iterations of the maps, the entropy, and the correlation function for the population densities. In Sec. IV we consider a long chain (101 sites) with periodic boundary condition, we calculate the spatial correlation function and fluctuation in population for an initially almost uniform distribution of individuals among the sites. Finally, Sec. V contains a summary and conclusions.

II. THE RANDOM MIGRATION MODEL AND POPULATION DYNAMICS

Let us consider a set of sites, $2M+1$ trees for instance, labeled as $-M, -M+1, \ldots, -1, 0, 1, \ldots, M$, containing a population $U_{m,n}$ of insects at site m and at time n. Initially, at time $n=1$, the *primordial site* has $U_{0,1} \neq 0$ individuals and all others have $U_{m \neq 0,1} = 0$. At the following time, $n=2$, any individual have either already emigrated to the nearest neighbor tree [with probability p (q) to the right (left) tree] or did stay on the same tree with probability $1-p-q$. The probability of having emigrated to a farther tree, by hopping the nearest ones, is zero. This is the random walk model (the continuous version is the diffusion equation), which is linear. Assuming that at each site the population varies dynamically, then the $(2M+1)$-dimensional map is given by

$$U_{m,n+1} = pU_{m+1,n} + qU_{m-1,n} + R_m(\cdot)(1-p-q)U_{m,n},$$

$$m = -M, \ldots -1, 0, 1, \ldots M, \tag{3}$$

which is a set of $2M+1$ coupled equations to be solved simultaneously, with $0 \leqslant p, q \leqslant 1$, and $p+q \leqslant 1$. The population growth function R_m represents the on-site variation of the population, affecting all the individuals that are not migrating, in all the sites. For example, R_m could represent the ratio between reproduction and death rates at each site. We

shall consider three situations: (i) The function R_m assumes a constant value r for all trees, (ii) R_m depends on the total population, $R(P_n)$, where $P_n=\Sigma_{m=-M}^{M}U_{m,n}$, (iii) R_m depends on the population of each tree, $R_m(U_{m,n})$.

Comparatively, in Ref. [12] the migration is assumed occurring from any site to any other site with probability p, according to the following linear equation

$$(1-p)U_{m,n}+\frac{p}{2M+1}\sum_{m=-M}^{M}U_{m,n}\equiv\mathcal{M}U_{m,n},$$

where $\mathcal{M}$ is the operator representing migration and the size of each population changes according to the map

$$U_{m,n+1}=f(\mathcal{M}U_{m,n}). \tag{4}$$

In our approach, differently from Ref. [12], we consider that the population at each site m changes at time $n+1$ due to an intrinsic process, moreover any site may lose (gain) individuals due to emigration (immigration) to (from) nearest neighbors only. For case (i), $r=1$ means that the total population P_n remains constant, $P_{n+1}=P_n$, and asymptotically the random walk makes the initial population, at the primordial tree, to distribute equally likely between all other trees. For a non-negative r the total population will vary with time according to equation

$$P_{n+1}=[(p+q)(1-r)+r]P_n, \tag{5}$$

which is typically Malthusian since the factor in brackets is a positive constant, although it depends on three parameters, each having its own physical meaning. If $p+q=1$, each and every individual in a tree forcefully emigrates to a neighbor tree, therefore $P_{n+1}=P_n$, the total population remains constant because the process describes only the migration of the individuals that will hop from tree to tree until equilibration is attained. Asymptotically, every tree will accommodate the same number of individuals. In case (ii) we suppose that R depends on the total population P_n, therefore Eqs. (3) and (5) become

$$U_{m,n+1}=pU_{m+1,n}+qU_{m-1,n}+R_m(P_n)(1-p-q)U_{m,n}, \tag{6}$$

$R_m(P_n)=R(P_n)$ is the same for each tree and

$$P_{n+1}=\{(p+q)[1-R(P_n)]+R(P_n)\}P_n. \tag{7}$$

The fixed point is determined by the equation $R(P_*)=1$, irrespective of the value of $p+q$. If there is no migration, $p+q=0$, Eq. (7) reduces to Eq. (1) describing the dynamics of a single site. In the following we will consider a specific model for $R(P_n)$ or $R_m(U_{m,n})$.

A. Ricker's model

In order to analyze the effects of the migration on the dynamics of the population we have adopted the two-parameter model proposed by Ricker in 1954 to describe the dynamics of the salmon population of the Pacific coast of Canada [19]. This is represented by the map (1), with

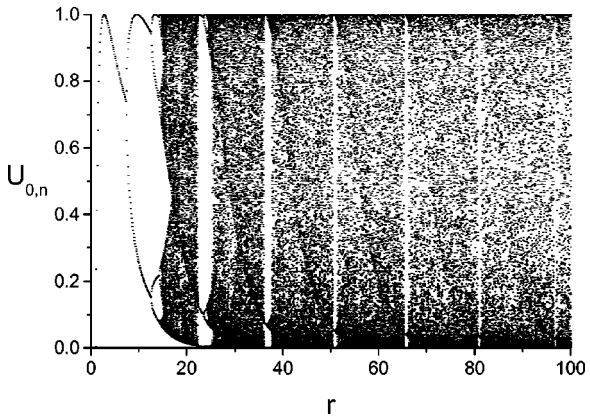

FIG. 1. Normalized bifurcation diagram for $p=0$ (no migration) representing the population density at the primordial site. For $0<r<1$ the population tends to its extinction; for $1\leqslant r<e^2$ there is a single fixed point, the population attaining a stable equilibrium; at $r=e^2\simeq 7.39$ a bifurcation occurs, the population oscillates between two values (period-2 oscillation); for higher values or r there is a period-4 oscillation and so on. Doubling the periods of oscillation goes on until $r\cong 14.2$; beyond this value the population density oscillates chaotically. The growth rate parameter r is dimensionless.

$$R(P_n)=re^{-P_n/K}. \tag{8}$$

Interestingly, Ricker's map is also able to describe epidemiological dynamics, it was found to fit the data of incidence of measles and other epidemics [20]. In Eq. (8), K is a saturation constant of the environment and r is the maximum per generation rate at which the population multiplies or simply the growth rate of the species. The map $P_{n+1}=P_nR(P_n)$ have a fixed point $P_*=K\ln r$ (besides the trivial one $P_*=0$), eigenvalue $\lambda=1-\ln r$, and point of maximum $P_m=K$; for $K>0$ only $r>1$ has a physical meaning, therefore $P_*>P_m$. Thus P_* will remain a stable fixed point as long as $-1<\lambda<0$ (or equivalently $1<r<e^2$). Setting $K=10\,000$ and varying r in the interval $(0,\ 100)$, one sees in Fig. 1 the bifurcation diagram ($P_n\times r$, discarding a transient time) displaying the following characteristics: for $0<r<1$ the population tends to its extinction ($P_*=0$), for $1\leqslant r<e^2$, P_n has a single fixed point, the population attaining a stable equilibrium ($P_*=K\ln r$), at $r=e^2\simeq 7.39$ a bifurcation occurs, meaning that for $e^2\leqslant r\lesssim 12.4$, P_n oscillates alternatively between two values (period-2 oscillation), for higher values or r it will show a period-4 oscillation and so on, the doubling of oscillation periods goes on until $r\cong 14.2$; beyond this value P_n oscillates chaotically. So, the bifurcation diagram shows that the map goes chaotic by period doubling. Periodic oscillations of populations are found in nature, for instance, in population of lemmings [21] and in the potato beetle *leptinotarsa* of Colorado [8]; chaotic oscillations seem to occur in the Canadian lynx [22] and in the ''gipsy moth'' *limantria dispar* [23].

B. Growth function in all sites depending on local population density

We will assume isotropic random migration, $p=q$, meaning that the initial population in the primordial site diffuses

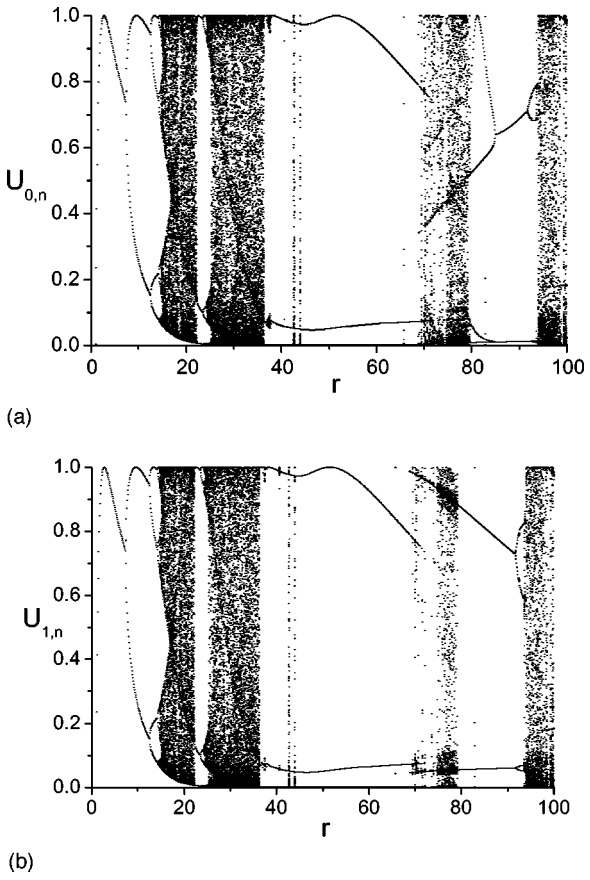

FIG. 2. Same as Fig. 1 but for $p=0.000\,01$ and case (ii). (a) Tree $m=0$; (b) for trees $m=1,-1$, the bifurcation diagram is the same due to symmetry. The migration is isotropic ($p=q$), initially $U_{0,0}=1$ and $U_{\pm 1,0}=0$. Comparing with Fig. 1, the chaotic oscillations are suppressed for many values of r, being replaced by period-2 or period-4 oscillations. The diagrams show similar but not identical behavior, the population is initially present in the primordial site only.

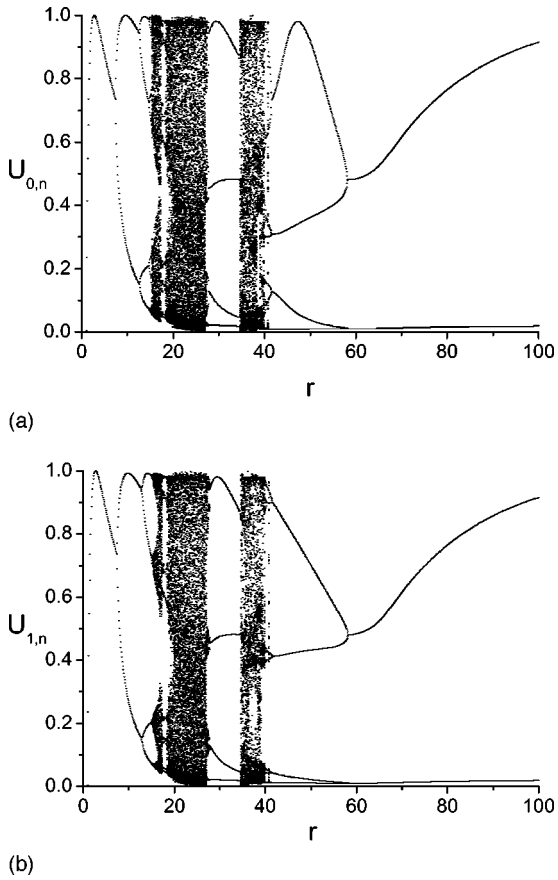

FIG. 3. Same as Fig. 2 but with a higher-migration rate, $p=0.01$. (a) Tree $m=0$; (b) trees $m=1,-1$. Beyond $r\approx 42$ the chaotic oscillation is suppressed. Period-4 and then period-2 oscillations substitute the chaotic oscillations of Fig. 1.

to other sites. Should we have set $p\neq q$ there would be a drift velocity proportional to $p-q$ [the continuous version of Eq. (3) with $R_m(\cdot)=r$, constant, is a Fokker-Planck equation] with the center of the ''wave-packet'' moving to the left (right) for $p>q(p<q)$. The presence of a population dependent growth function $R_m(\cdot)$ in Eq. (3) changes the purely diffusive motion of the individuals through the sites, this term gives rise to a wave front of individuals advancing symmetrically (when $p=q$) to the left and to the right out from the primordial site. We return to this point in Sec. IV.

We also consider periodic boundary conditions for a system of three trees, $M=3$, $m=-1,0,1$, and $R_m(U_{m,n})$ given by Eq. (8). As can be seen in Fig. 2(a) ($U_{0,n}$) and 2(b) ($U_{1,n}\equiv U_{-1,n}$) (to be compared with Fig. 1) the effects on the bifurcation diagram are significant even for a small migration rate, $p=0.000\,01$. The chaotic region becomes partially suppressed, chaos being confined to some narrow strips of values of r and for $r>45$ the population oscillates again with period 4 and then with period 2 for a larger r. The suppression of chaos increases with higher values of the migration-rate parameter: for $p=0.01$, see Figs. 3(a)–3(b), and for $p=0.3$, see Fig. 4, where the chaotic oscillations are totally suppressed, for $r\gtrsim 14.2$ the population oscillates with period 2.

C. Growth function in the primordial site only

Now we go through the case when the individuals of a population reproduce or die in the primordial tree only

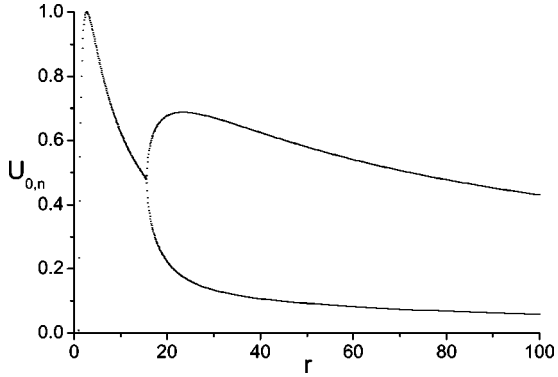

FIG. 4. Same as Fig. 2 but with a higher-migration rate, $p=0.3$. The map is for tree $m=0$, the others are quite similar. The chaotic oscillations are completely suppressed, replaced by a period-2 oscillation.

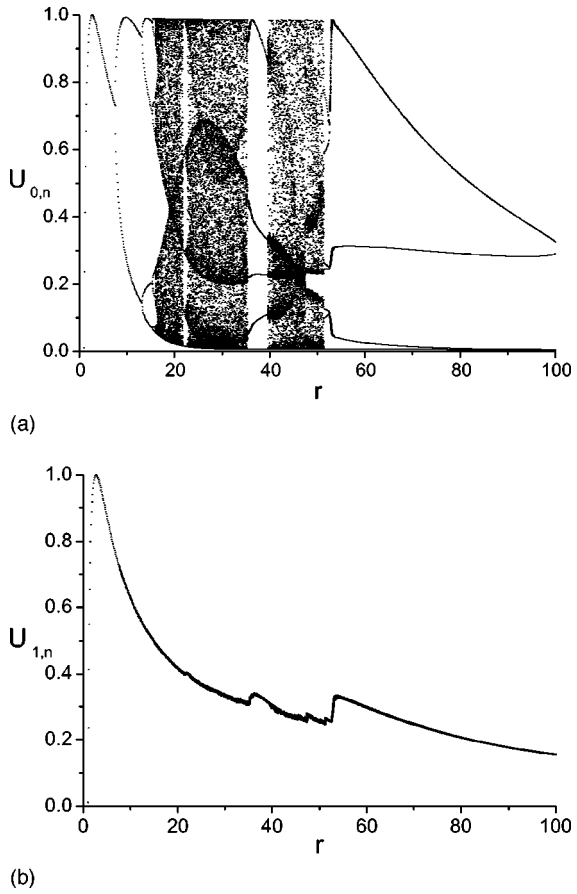

FIG. 5. Same as Fig. 1 but with $p=0.01$ and case (iii), when the growth function depends on the primordial site population only, Eqs. (9). (a) For tree $m=0$ the chaotic oscillations persist for higher values of r than for case (ii), compare with Fig. 3, and period-4 oscillations dominate instead of period 2; (b) trees $m=1,-1$, quite differently from Fig. 3(b), the period n and chaotic oscillations are substituted by a dense and narrow interval of oscillations.

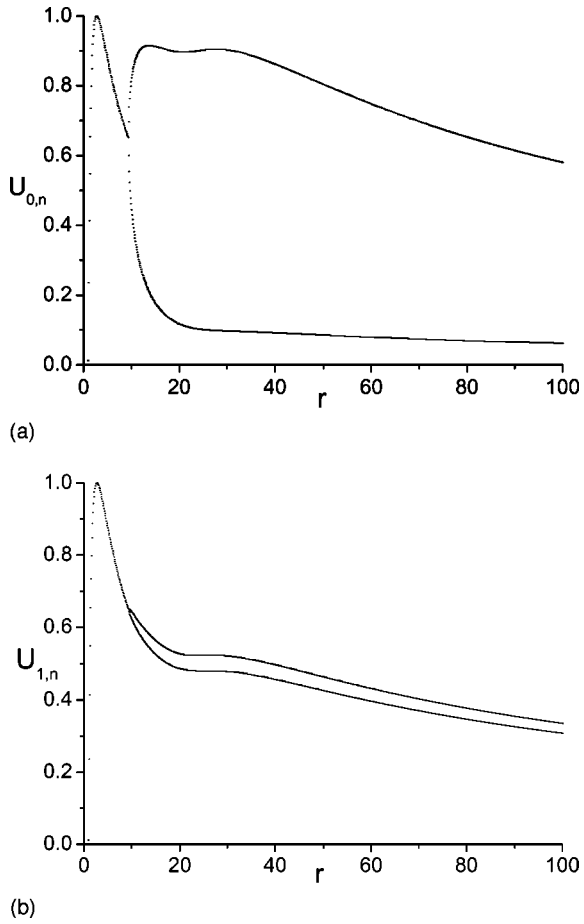

FIG. 6. Same as Fig. 5 but with $p=0.1$. For all trees one sees a period-2 oscillation; however, the gaps between population sizes are quite different: (a) tree $m=0$ and (b) trees $m=\pm 1$. In the latter, the population shows a higher stability. In both figures the bifurcation occurs at the same value of r.

$[R_0(U_{0,n})\neq 0$ and $R_{m\neq 0}(U_{0,n})=1]$, the other trees becoming populated only due to immigration. Again, we consider three trees and periodic boundary conditions. We did not find appreciable qualitative changes for a greater number of trees, however we will consider a long chain in Sec. IV, where we analyze the spatial correlation and population fluctuations. The set of equations is

$$U_{-1,n+1}=p(U_{0,n}+U_{1,n})+(1-2p)U_{-1,n},$$

$$U_{0,n+1}=p(U_{1,n}+U_{-1,n})+re^{-U_{0,n}/K}(1-2p)U_{0,n}, \quad (9)$$

$$U_{1,n+1}=p(U_{0,n}+U_{-1,n})+(1-2p)U_{1,n},$$

all trees have the same fixed point, $U_{m,*}=K\ln r$, and the global population stabilizes (period 1) at $P_*=(2M+1)K\ln r$. In Figs. 5(a) and 5(b), we present the bifurcation diagrams of $U_{0,n}^{-}$ and $U_{\pm 1,n}^{-}$ for $p=0.01$. In Fig. 5(a) the chaotic oscillations persist for higher values of r than for case (ii), compare with Fig. 3(a), and period-4 oscillations dominate instead of period 2. In Fig. 5(b), trees $m=\pm 1$, the diagram is quite different than that in Fig. 3(b), the period n and chaotic oscillations are substituted by a dense interval of oscillations, a narrow band of fixed points (for each value of r), showing very small fluctuations. In Fig. 6(a) and 6(b), for $p=0.1$ the chaotic oscillations are totally suppressed and substituted by period-2 oscillations. These oscillations also occur in sites $m=\pm 1$, although for any value of r the gap between the two allowed population densities is strongly reduced.

III. HIGHER-ORDER MAP ITERATIONS, ENTROPY, AND CORRELATION FUNCTIONS

In this section we discuss the effects of the random migration on the population dynamics by looking at higher-orders map iterations, entropy, and correlation function.

Initially, we consider the first three iteration maps, $U_{0,n+1}\times U_{0,n}$, $U_{0,n+2}\times U_{0,n}$, $U_{0,n+3}\times U_{0,n}$; in the case of no migration, $p=0$, and for highly chaotic oscillations ($r=20$), the calculated numerical points will fall (distributed almost evenly) on the continuous analytical curve $f(x)$, where $U_{0,n+1}=f(U_{0,n})$. This shows that a chaotic time or numerical series provides essential information on the func-

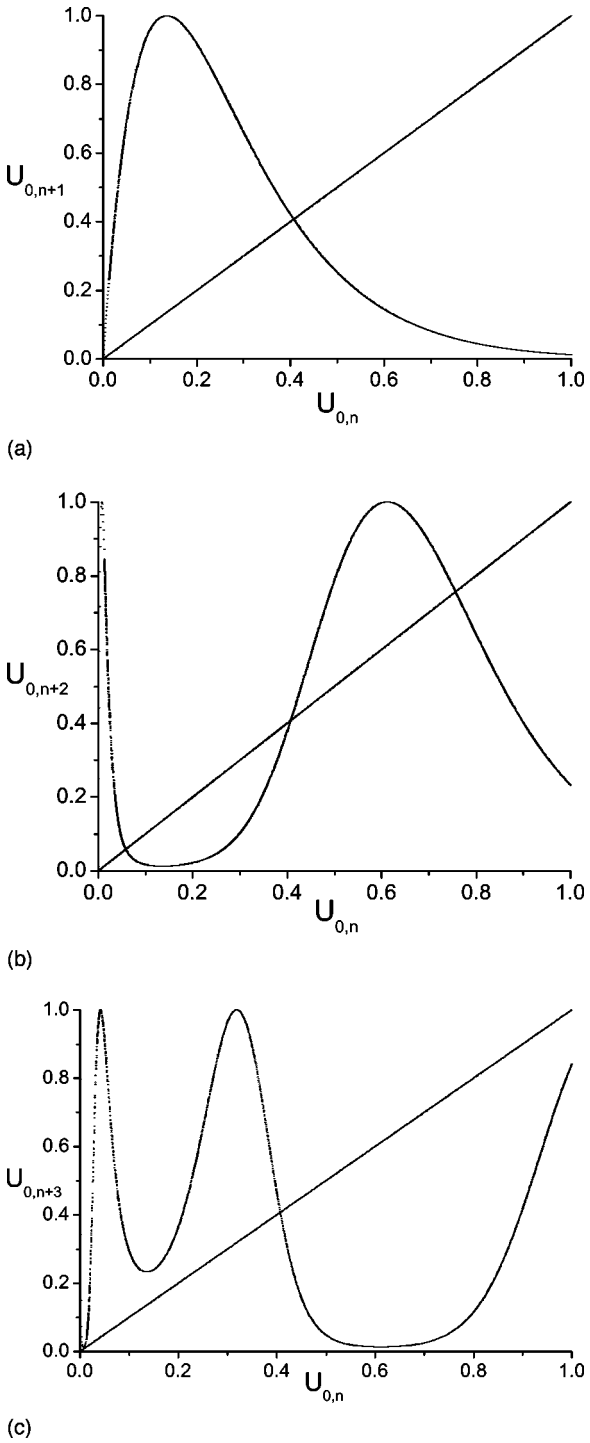

FIG. 7. The maps of the central tree for $p=0$; (a) $U_{0,n+1} \times U_{0,n}$, (b) $U_{0,n+2} \times U_{0,n}$, and (c) $U_{0,n+3} \times U_{0,n}$.

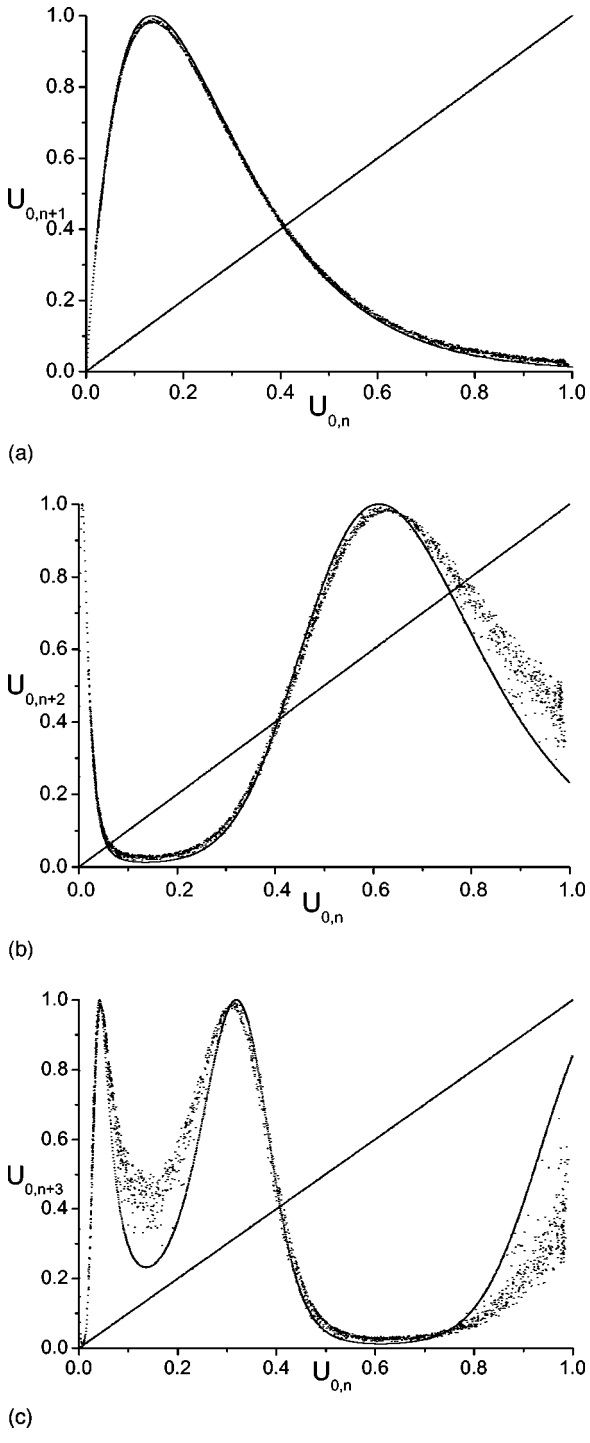

FIG. 8. Same as in Fig. 7 but now $p=0.01$. Note that due to migration there occurs a scattering of the numerical points nearby the analytical $p=0$ curve.

tional form of an unknown map f, which could not be possible if the oscillations were periodic (only two points for a period-2 oscillation, four points for a period-4 oscillation, etc.). In Figs. 7(a)–7(c) we set $r=20$ and considered 2000 points after having discarded a transient (500 points), the numerical points fall on the analytical curves of the maps $y_1=f(x)$, $y_2=f(f(x))=f^{(2)}(x)$, and $y_3=f(f(f(x)))=f^{(3)}(x)$, respectively. As we increase the order of the iterations, the distribution of the points become more sparsely distributed, because the number of generated points is fixed while the lengths of the curves increase.

For $r=20$ and a small migration rate, $p=0.01$, the maps shown in Figs. 8(a)–8(c) can be compared with those of Fig. 7(a)–7(c). Although in the first iteration map, Fig. 8(a), the numerical series shows a slight deviation from the analytical curve, the second and third iterations show more significant deviations. Two effects can be perceived in the maps: (i) the

numerical points do not fall, precisely all, on the analytical curves, instead they are scattered in the vicinity and (ii) the points do not distribute symmetrically around the analytical curve but either above or below. The information about the functional forms of $f(x)$, $f^{(2)}(x)$, $f^{(3)}(x)$, etc. could not be retrieved from a time series with the same accuracy as for the $p=0$ case, because information is partially lost due to the random migration. Thus, if one wants to derive the functional expression of a map from a numerical or experimental time series, care is recommendable because, if randomness is present in a dynamical process the lost information prevents the retrieval of the function $f(x)$. These peculiarities of the numeric series suggest the use of an entropy function to quantify the information loss.

A. Entropy

We want to measure the ''overlap'' of the $p\neq 0$ numerical series with the $p=0$ analytic map, so we introduce a modified version of the Kolmogorov entropy (K entropy) [24], in order to quantify the information loss due to the random migration. The definition is based on square deviations. For a map $x_{n+1}\times x_n$, where $x_{n+1}=f(x_n,r,p)$, $n=1,2,\ldots N$ (N points after the transient, r is a parameter), one divides the domain of x into N cells (intervals) of equal width, defined as $I_i\equiv(x_{i-1},x_i]$ with $i=1,2,3,\ldots N$. For a discrete time series (numerical or experimental), we denote as $[x_n^{(i)},x_{n+1}^{(i)}]$, the pair of coordinates of the first numerical point of the series with $x_n^{(i)}$ falling into cell I_i, the succeeding points falling into this same cell are not considered since they do not contribute with additional information. Then we introduce the quantity

$$\Delta_i(r,p,N)=\frac{\left(1-\dfrac{x_{n+1}^{(i)}}{f(x_n^{(i)})}\right)^2}{\displaystyle\sum_{i=1}^{N}\left(1-\frac{x_{n+1}^{(i)}}{f(x_n^{(i)})}\right)^2},$$

which gives the normalized deviation of a subset of points of a discrete numerical series, with respect to a function f, at the points $x_n^{(i)}$. One notes that $\Delta_i(r,p,N)$ (in the interval $[0,1]$) is a weight associated with each cell, with $\Sigma_{i=1}^{N}\Delta_i=1$. In case of no random migration ($p=0$) all points fall on the curve $f(x)\times x$, for the N_0 ''occupied'' cells the weights are $\Delta_i=0$ whereas $N-N_0$ ''empty'' cells have weight $1/(N-N_0)$. For instance, for a value of r leading to a single fixed point (period 1), the cell to which it belongs has weight $\Delta_i=0$, whereas all $N-1$ other cells have weight $1/(N-1)$; for r showing period-2 oscillation the two corresponding cells have weights $\Delta_i=0$ while all other $N-2$ cells have weight $1/(N-2)$, and so on. Even in the more chaotic region there may be empty cells. So we define the entropy of the numerical series with respect to the function f as

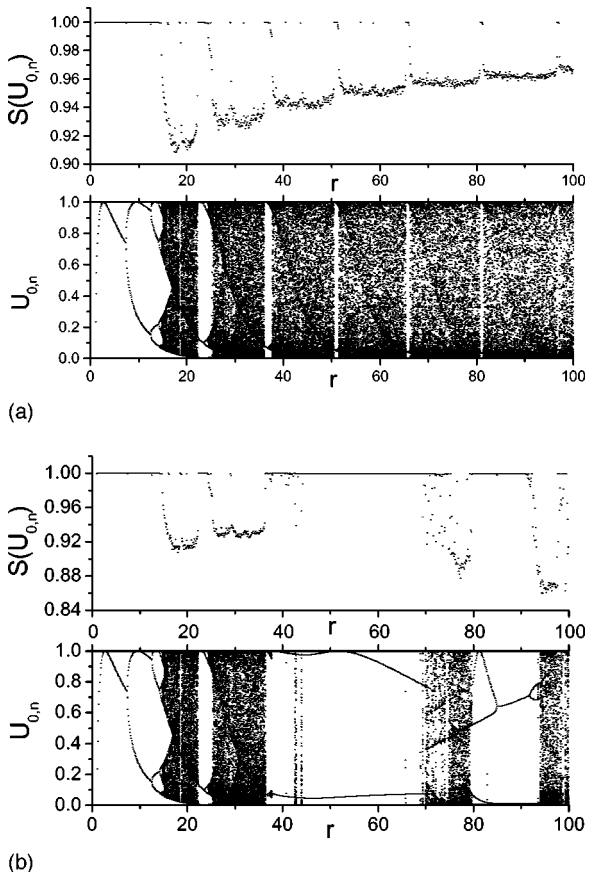

FIG. 9. The upper sides of (a) and (b) stand for the entropy $S_{U_{0,n}}$ while the lower sides (bifurcation diagrams) were inserted for the sake of comparison. (a) shows that in a chaotic region the entropy is lower for a more uniform distribution of the numerical points (for each value of r), so a higher coincidence with the analytical curve. For values of r corresponding to blank windows (a single fixed point or period-n oscillations in the lower part of the figure) the entropy attains its higher values because the map gives very few distinct points on the analytical curve. (b) is for $p=0.000\,01$, for many values of r the information that could be available from the map is completely lost.

$$S_f(r,p)=-\lim_{N\to\infty}S_f(r,p,N)\equiv-\lim_{N\to\infty}\frac{\displaystyle\sum_{i=1}^{N}\Delta_i\ln\Delta_i}{\ln(N-1)}.$$

For $p=0$ and period 1 the entropy attains its highest value, $S_f(r,0)=1$, meaning that the numerical series does not contain any meaningful information about the function f, all points falling on a single point of the analytical curve. In the ideal case where all N cells are ''occupied,'' all the weights $\Delta_i=0$, the entropy $S(r,0)=0$, so the numerical points become uniformly distributed on f and the information is maximum. Upper sides of Figs. 9(a) ($p=0$) and 9(b) ($p=0.000\,01$) stand for the entropy, $S_{U_{0,n}}\times r$ and the bifurcation diagram (lower side) was inserted for the sake of comparison. In Fig. 9(a) the entropy is lower for a more uniform distribution of points in the chaotic regions (for each value of r), meaning that coincidence with the analytical curve (the

map) is more faithful. For a parameter r corresponding to a single fixed point or period-n oscillation (the blank windows in the lower side of the figure) the entropy attains its higher values because the map gives very few distinct points for reproducing the analytical curve. When $p \neq 0$, Fig. 9(b), for many values of r a bunch of information is lost since the original chaotic oscillations become regular. From this we conclude that if some process produces a chaotic time series a faithful reconstruction of the function f by any method is not guaranteed if randomness or diffusion is present in the process.

B. Time correlation functions

The numerical series allows us to calculate the correlation between the on-site population density at different times (autocorrelation) or between different trees at the same or at different times (mutual correlation). This quantification is another tool to analyze the effect of migration on the population dynamics in each site.

The normalized correlation function is defined as

$$C(U_{m1},U_{m2},l)=\lim_{N\to\infty}\frac{N\sum_{n=1}^{N-l}U_{m1,n}U_{m2,n+l}-\left(\sum_{n=1}^{N-l}U_{m1,n}\right)\left(\sum_{n=1}^{N-l}U_{m2,n+l}\right)}{\sqrt{\left[N\sum_{n=1}^{N-l}(U_{m1,n})^2-\left(\sum_{n=1}^{N-l}U_{m1,n}\right)^2\right]\left[N\sum_{n=1}^{N-l}(U_{m2,n})^2-\left(\sum_{n=1}^{N-l}U_{m2,n}\right)^2\right]}}. \tag{10}$$

These correlations quantify the effects of the random migration on the ''memory'' of the time series, the parameter l is the time distance between iterations for the same ($m1=m2$) or different trees ($m1\neq m2$) (N should be quite large to allow stability). For $r=10$, the map presents a period-2 oscillation (the populations are perfectly correlated) and the ''memory time'' is quite large. However, for $r=20$, the oscillations are highly chaotic, in Figs. 10(a)–10(h) we present the plots of the autocorrelation function $C(U_0,U_0,l)$, for $p=0.0$, 0.0001, 0.001, 0.0015, 0.01, 0.011, 0.012, 0.013, respectively. The numerical points are linked by the solid lines while the dotted lines link their absolute values $|C(U_0,U_0,l)|$. One notes that the autocorrelation function does not decay monotonically, as long as the chaotic oscillations persist (for $p<0.013$), the envelope exhibits an oscillatory damping. For highly chaotic oscillations, $p=0.0$, 0.0001, the pattern of damped oscillations of the envelope is similar to a spherical Bessel function, $j_0(x)$, and with increasing p the chaotic oscillations become suppressed, displaying a smoothed envelope. In the interval, $p\simeq 0.012-0.013$ [Figs. 10(g)– 10(h)] a transition occurs, the correlation time suddenly increases (becoming quite large) so that the chaotic oscillations are replaced by regular ones; this shows the sensibility of the correlation time to small changes in p.

We do not present the plots for the autocorrelation function $C(U_1,U_1,l)$ and mutual correlation $C(U_0,U_1,l)$, since we did not find any new interesting feature.

IV. LONG 1D CHAIN

We now consider the asymptotic population distribution for a ''long'' chain of sites, $M=50$ (101 sites). In Figs. 11 and 12, we present the bifurcation diagrams (sites $m=0$ and $m=\pm 1$) to be compared to Figs. 2 and 3, respectively, for the same set of parameters. Besides few additional regions of chaos, the diagrams present evident similarity, the same kind of resemblance occurs with other diagrams, meaning that for the same value of p, asymptotically the bifurcation diagrams change weakly with M.

We analyze the spatial correlation of the populations considering, first, the growth function R_m acting in *all* sites, Eqs. (3), for $r=20$. In Fig. 13 we show the plots of

$$C(j,r,p)=\lim_{n\to\infty}\frac{(2M+1)\sum_{m=-M}^{M}U_{m,n}U_{m+j,n}-\left(\sum_{m=-M}^{M}U_{m,n}\right)^2}{(2M+1)\sum_{m=-M}^{M}(U_{m,n})^2-\left(\sum_{m=-M}^{M}U_{m,n}\right)^2} \tag{11}$$

for $p=0.2$, 0.3, 0.4, when the asymptotic stability is attained. However, n odd and n even times show different behavior, at n odd times (bullets) the populations show a stronger correlation than at n even times (squares), this difference occurs because the populations oscillate with period 2 at two different densities. Second, for higher diffusion parameter, $p=0.3,0.4$, when chaotic regime is already suppressed, the correlation functions acquire a regular behavior independently of p. For $j<26$, the correlation is stronger for even j than for odd j, this trend being reverted at $j=27$, the *transition point*, when sites having odd-j separation become more strongly correlated. While the even-j correlation decreases monotonically with increasing j, for odd j, the correlation begin increasing with j, then shows a stability in the interval $j\approx 11-39$, then decreases returning to its initial value. This behavior occurs for n even or n odd times, however, it is much more evident at n even times.

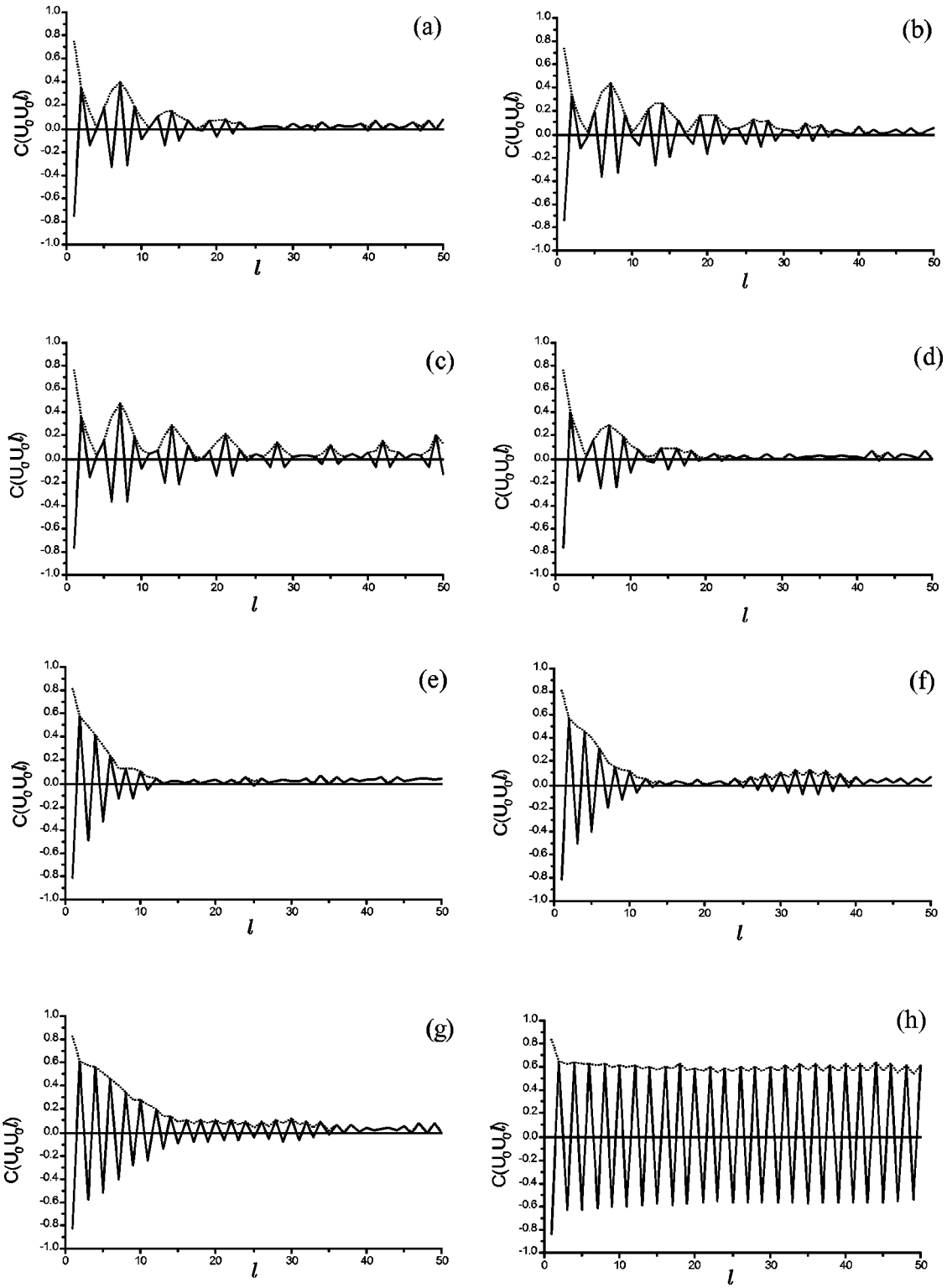

FIG. 10. Autocorrelation function for the primordial site, $r=20$ and (a) $p=0$, (b) $p=0.0001$, (c) $p=0.001$, (d) $p=0.0015$, (e) $p=0.01$, (f) $p=0.011$, (g) $p=0.012$, (h) $p=0.013$. The solid lines link the numerical points and the dotted lines link their absolute values. For $p=0.013$ the chaotic oscillation vanishes, being replaced by a regular one and the autocorrelation function does not damp with increasing l.

When growth is allowed in the primordial site only, the correlation functions show a different behavior, see Fig. 14, to be compared to the previous case (Fig. 13). Now there is no more strong differences between even j and odd j, the correlations fit on a single curve, although difference continues between n even and n odd times for $p=0.1$, 0.2, due to period-2 oscillation in populations, but not for $p=0.3$, 0.42 since the populations present a single fixed point. A *transition point* occurs only for $p=0.1$ not appearing for higher values of p.

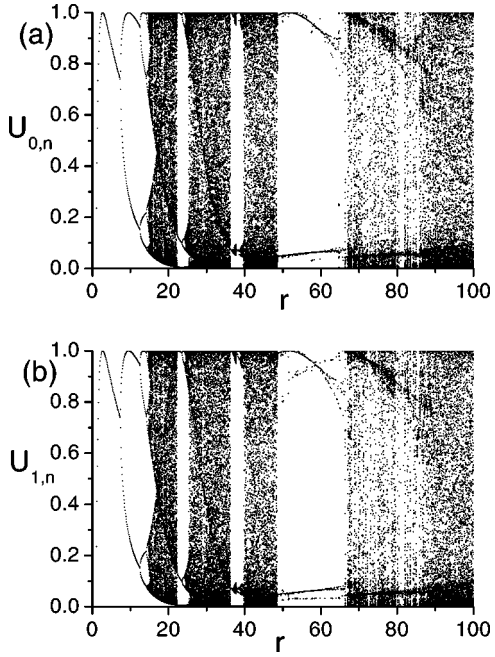

FIG. 11. Compared to Fig. 2, here $M=50$ for the same set of parameters, (a) $m=0$, (b) $m=\pm 1$. Qualitatively the bifurcation diagram shows the same behavior as for $M=3$.

Now we analyze the population fluctuations when all sites are initially ($n=1$) populated, however showing a slight difference in the number of individuals between each other: we set 5000 individual in the primordial site ($U_{0,1}$), the consecutive sites having, sequentially, a decrease of ten individuals ($U_{\pm 1,1}=4990, U_{\pm 2,1}=4980, \ldots, U_{\pm 50,1}=4500$). Considering first the case when the growth function acts on all sites, we

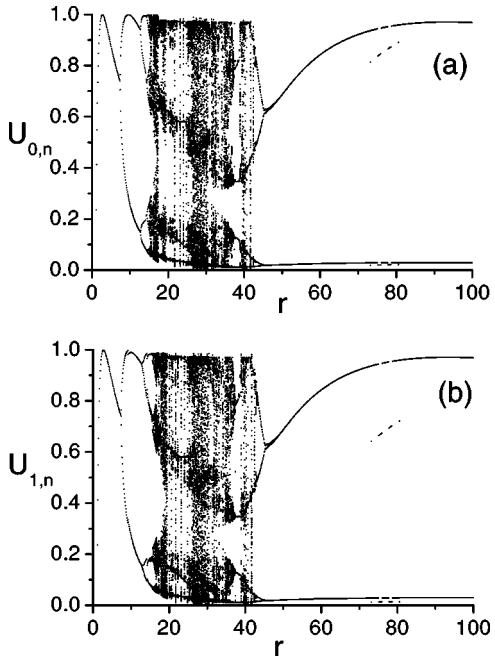

FIG. 12. Compared to Fig. 3, here $M=50$, for the same set of parameters, (a) $m=0$, (b) $m=\pm 1$. Qualitatively the bifurcation diagram shows the same behavior as for $M=3$.

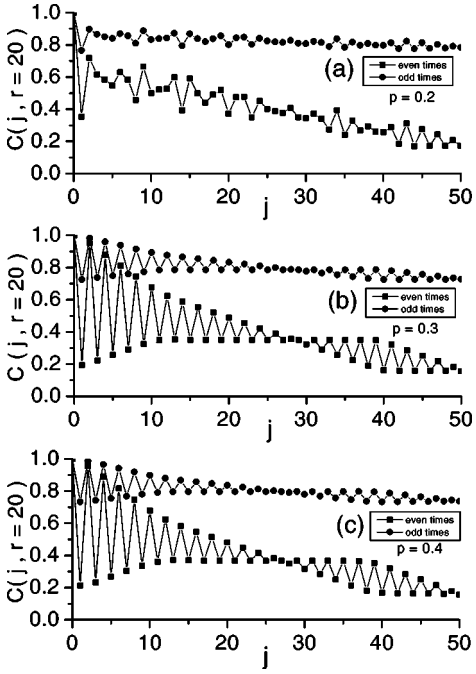

FIG. 13. The spatial correlation function, Eq. (11), as a function of intersite distance j, in arbitrary units, when growth occurs in all sites and $M=50$. (a) $p=0.2$, (b) $p=0.3$, (c) $p=0.4$. Asymptotic even (squares) and odd (bullets) times show different behaviors. Correlations for even and odd values of j show different trends; in (b) and (c), at $j=26$, there is a transition point where correlation strength changes.

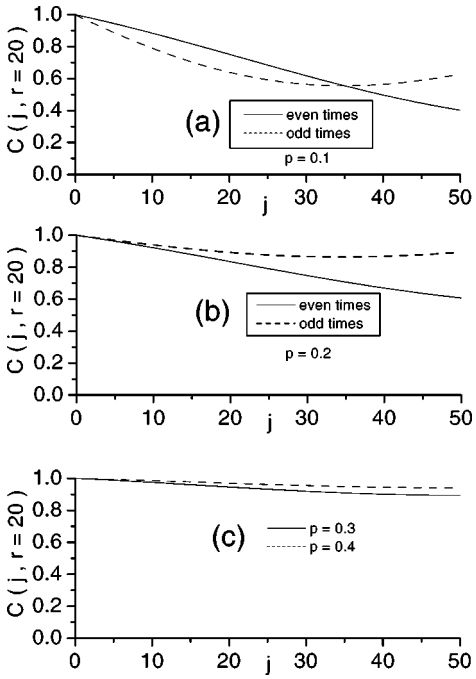

FIG. 14. The spatial correlation function, Eq. (11) as function of intersite distance j, in arbitrary units, when growth is allowed in the central site only and $M=50$. (a) $p=0.1$, $p=0.2$, (c) $p=0.3$, 0.4. In (a) and (b) asymptotic even (solid line) and odd (dash line) times show different behaviors, while in (c) there is no more difference.

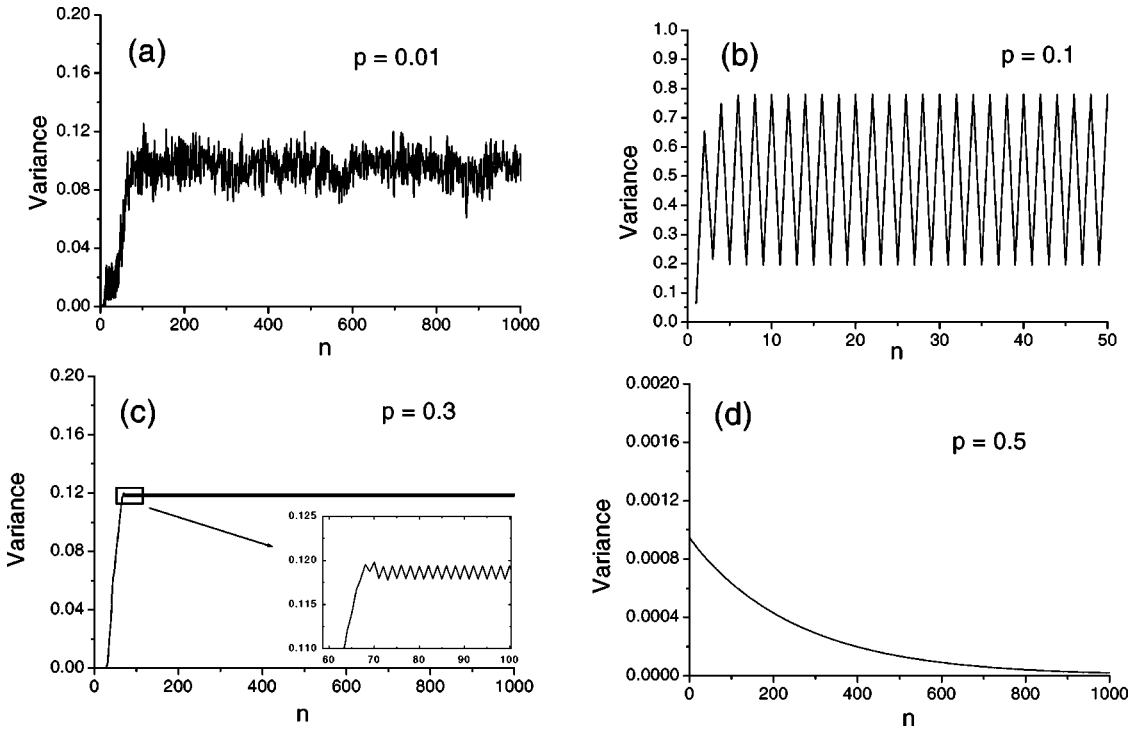

FIG. 15. Variance of site populations as a function of time n in arbitrary units, when growth occurs in all sites and $M=50$. (a) $p=0.01$, chaotic regime; (b) $p=0.1$, period-2 oscillation; (c) $p=0.3$, period-2 oscillation; (d) $d=0.4$, growth is completely suppressed, fluctuations die out, only migration is allowed.

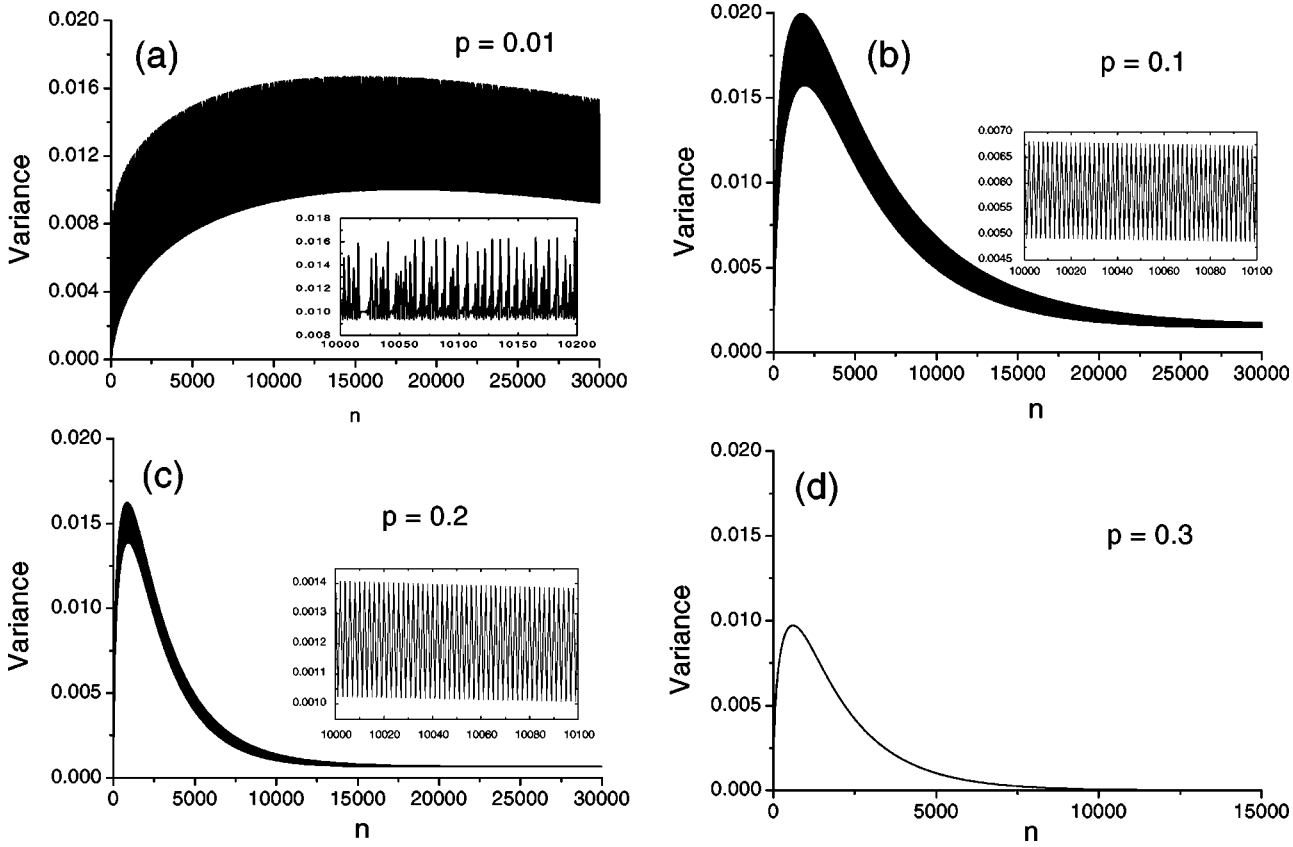

FIG. 16. Site populations variance as a function of time n in arbitrary units, when growth is allowed in the primordial site only and $M=50$. (a) $p=0.01$, still in the chaotic regime; (b) $p=0.1$, period-2 oscillations; (c) $p=0.2$, period-2 oscillation, oscillation amplitude is reduced; (d) $d=0.3$, no more oscillations, each site attains a single fixed point (period 1).

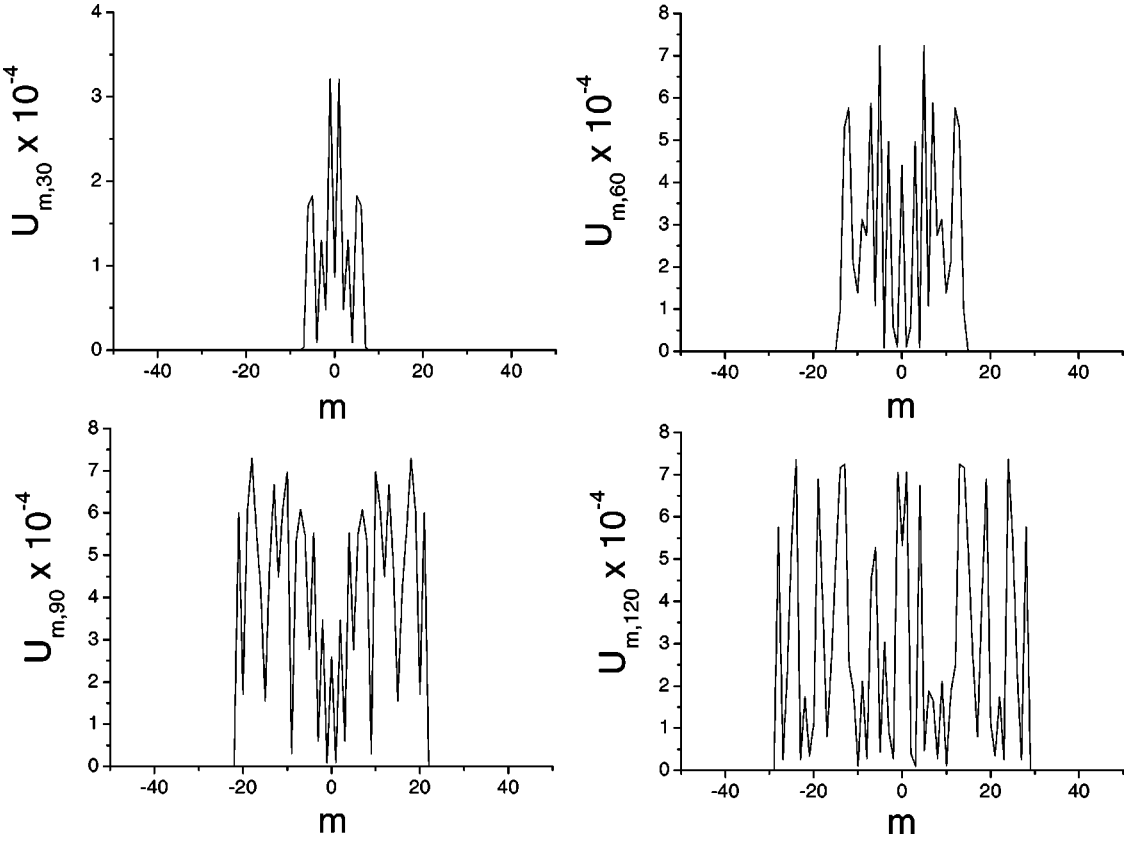

FIG. 17. Population distribution among the sites, when growth is allowed in all sites, for diffusion parameter $p=0.000\,01$ and for times $n=30$, 60, 90, 120 (in arbitrary units). One sees the formation of a traveling sharp wave front.

present in Fig. 15 the plots of the variance as function of time or population fluctuations for $r=20$ and different values of p, with population sizes properly normalized. For $p=0.01$, Fig. 15(a), the population is still in the chaotic regime, after a transient time fluctuations stabilize around 0.1, showing a narrow chaotic amplitude oscillation. For $p=0.1$ [Fig. 15(b)], the populations do not oscillate anymore chaotically, after a transient the fluctuations become regular with wide amplitude, taking alternating fixed values for even and odd times. The same occurs for $p=0.3$ although now the fluctuation amplitude is quite narrow [see insertion in Fig. 15(c)]. For $p=0.5$, the individuals only migrate, they do not reproduce or die, the whole population remains constant; the initial variance of the population was quite small and the fluctuations die out asymptotically, differently for the cases $p<0.5$.

When the population reproduces in the primordial site only, the fluctuations show a quite different quantitative and qualitative behavior. Examining Figs. 16(a)–16(d), first it is worth noting that much longer times were considered in order to look for stabilization of the fluctuations. For $p=0.1$, Fig. 16(a) the chaotic regime is still present and until $n=30.000$ the wide fluctuations did not stabilize yet, however after going through a maximum there is a tendency of reduction. For $p=0.1$, 0.2, Figs. 16(b)–16(c), the fluctuations become narrower and regular, then stabilizing asymptotically, however they show that populations of the sites oscillate with period 2. For $p=0.3$, Fig. 16(d), the variance shows the same trend, however populations present a single fixed point.

From the analysis of the fluctuations we conclude that when growth occurs in all sites the fluctuations stabilize in a much shorter time than if growth is allowed in the primordial site only, even if growth (Ricker's map) occurs in the chaotic regime. In the latter case, the individuals should make a longer ''walk'' to return to the primordial site in order to reproduce for a second, third,... time, whereas in the former case either remaining on the same site or emigrating to a neighboring one, the reproduction is possible, therefore stability in fluctuations is more rapidly attained.

We analyze the possible existence of a travelling wave front of the individuals: when the growth function R_m acts in all sites, even for a very small diffusive parameter, $p=0.000\,01$, a sharp traveling wave front appears as can be seen in Fig. 17, where we plotted the populations during the transient regime at four times, $n=30$, 60, 90, 120. From the figure, one estimates that the wave front advances at a nearly constant speed of seven sites for each 30 units of time. Considering now that the population increases only in the primordial site, even for a much larger diffusion parameter, $p=0.2$, no wave front develops, only a diffusion pattern appears as seen in Fig. 18, where the curves correspond, from the inner to the outer, to times $n=100$, 200, 300, 400.

Thus one sees how Eq. (3) acts when growth occurs in all sites: diffusion (even very small) takes few individuals to the neighboring sites whereas the growth function acts by multiplying those (initial population at the site) at a high rate,

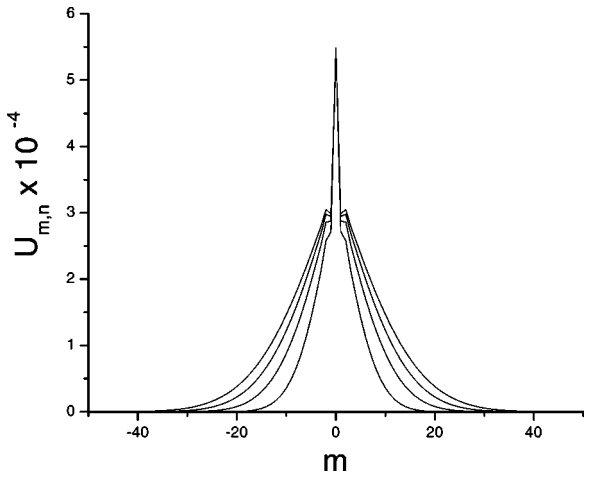

FIG. 18. Population distribution among the sites, when growth is allowed in the primordial site only, with diffusion parameter $p=0.2$. No wave front develops, only a diffusion pattern appears, and the curves correspond, from the inner to the outer, to times $n=100$, 200, 300, 400 (in arbitrary units).

thus creating a wave front that advances until all the available empty sites become occupied. This mechanism reminds Fisher's (partial differential) equation having a travelling wave front solution, which was proposed for explaining the spatial spread of a favored gene (a discussion is found in Ref. [5], Chap. 11). In the present case, as the wave front advances the number of individuals that populate the visited sites is neither uniform nor changes smoothly, strong oscillations show up due to the chaotic behavior of growth function.

When growth takes place in the primordial site only, the individuals that migrate to other sites are allowed to multiply only while returning to the primordial site, thus the diffusion motion prevails and no wave front is created.

V. SUMMARY AND CONCLUSIONS

In the present paper, we presented an analysis of the population dynamics of a generic species (insects) whose individuals are allowed to migrate randomly to nearest neighbors sites (trees for instance). We assumed that the population at each site varies dynamically according to Ricker's map. We essentially found that if the population in the primordial site presents chaotic oscillations, then, even for a small migration-rate parameter there is a tendency to chaos reduction. In certain instances it becomes suppressed, being replaced by period-2 or period-4 oscillations, depending on the value of the growth-rate parameter. The higher the migration rate the more rapidly the chaotic oscillations are suppressed. Thereafter we considered the case when the population increases dynamically only in the primordial site while on the other sites only migration is allowed. We found that for high migration rate chaotic oscillations are suppressed in all sites, being substituted by a period-2 oscillation; however the gap between the populations in the primordial site is quite larger than that in the neighboring sites. We also studied the influence of the migration rate on higher-order iterations of the maps, the entropy, and correlation functions.

Thereafter we considered a long chain of 101 sites, analyzing (a) the spatial correlation for both cases: when growth occurs in all sites and when it occurs on the primordial site only; and (b) the fluctuations in time of the populations, when initially all the sites are slightly differently populated, for both cases also. In the analysis of (a) we noted the occurrence of a transition in the correlation function between even and odd site distances, when the strength of the correlation is interchanged. In analyzing (b) we verified that the fluctuations stabilize in a much shorter time when growth is allowed in all sites instead of being on a single site only. We also verified that when growth is allowed in all sites a sharp travelling wave front develops, advancing toward unoccupied sites at a nearly constant speed. No such wavefront appears when growth is allowed in the primordial site, the individuals spread to the sites only by diffusion.

Finally, observing that chaotic oscillation in population dynamics is a phenomenon rarely observed in nature, with no unmistakable identification, we think that migration with adequate diffusion parameter could be one natural mechanism impeding its often occurrence.

ACKNOWLEDGMENTS

A.C. acknowledges financial support from FAPESP (São Paulo, SP, Brazil). S.S.M. acknowledges partial financial support from CNPq (DF, Brazil). We also acknowledge useful discussions with Professor A. Lichtenberg and Dr. J. De Luca.

[1] T. R. Malthus, *Population: The First Essay*, Ann Arbor paperbacks (The University of Michigan Press, Michigan, 1959).
[2] P. F. Verhulst, Mem. Acad. R. Belg. **18**, 1 (1845).
[3] R. M. May, *Theoretical Ecology. Principles and Applications* (Blackwell, Oxford, 1976).
[4] M. Kot and W. M. Schaffer, Theor Popul. Biol. **26**, 340 (1984).
[5] J. D. Murray, *Mathematical Biology*, Biomathematics Texts (Springer, New York, 1993).
[6] F. C. Hoppensteadt, *Mathematical Methods of Population Biology* (Cambridge University Press, New York, 1982).
[7] F. C. Hoppensteadt and C. S. Peskin, *Mathematics in Medicine and Life Sciences* (Springer-Verlag, New York, 1992).
[8] M. P. Hassell, J. H. Lawton, and R. M. May, J. Anim. Ecol. **45**, 471 (1976).
[9] P. Turchin and A. D. Taylor, Ecology **73**, 289 (1992).
[10] I. Suárez, Ecologic. Model. **117**, 305 (1999).
[11] M. Markus, B. Hess, J. Rössler and M. Kiwi, in *Chaos in Biological Systems*, Vol. 138 of *NATO Advanced Studies Institute, Series A: Life Sciences*, edited by H. Degn, A.V. Holden, and L.F. Olsen (Plenum Press, New York, 1987), p. 267.
[12] J. C. Allen, W. M. Schaffer, and D. Rosko, Nature (London) **364**, 229 (1993).

[13] P. Rohani and G. D. Ruxton, IMA J. Math. Appl. Med. Biol. **16**, 297 (1999).
[14] M. S. Magdon, Int. J. Mod. Phys. C **10**, 1163 (1999).
[15] R. B. de la Parra, O. Arino, E. Sanchez, and P. Auger, Math. Comput. Modell. **31**, 17 (2000).
[16] V. Padron and M. C. Trevisan, Math. Biosci. **165**, 63 (2000).
[17] T. Day, Am. Nat. **155**, 790 (2000).
[18] S. Charles, R. B. de la Parra, J. P. Mallet, H. Persat, and P. Auger, Ecologic. Model. **133**, 15 (2000).
[19] W. E. Ricker, J. Fish. Res. Board Can. **11**, 559 (1954).
[20] L. F. Olsen, in *Chaos in Biological Systems* (Ref. [11]), p. 249.
[21] C. Elton, *Voles, Mice and Lemmings: Problem in Population Dynamics* (Oxford University Press, Oxford, 1942).
[22] W. M. Schaffer, Am. Nat. **124**, 798 (1984).
[23] R. Breuer, Geol. J. **7**, 36 (1985).
[24] H. G. Shuster, *Deterministic Chaos* (Physik Verlag, Weinheim, 1988).